Bone Water in Human Tibiae with Subcritical Fatigue Damage: Integrating UTE-MRI and FT-NIR Toward New Biomarkers of Stress Fracture Risk

Cooper Rusch[1], Grant Belush[2], Glynn Gallaway[2], Ayishe Jin[2], Peter Jalaie[3], Wikum Bandera[3], Thomas Siegmund, PhD [2], Rachel Surowiec, PhD[1,3]

[1] Indiana University School of Medicine, [2] Purdue University School of Mechanical Engineering, [3]Purdue University School of Biomedical Engineering
cnrusch@iu.edu

Disclosures: None

INTRODUCTION: Stress fractures account for nearly 20% of all sports medicine injuries and 10% of all orthopedic injuries, particularly along the tibial shaft, can lead to prolonged pain, disability, and recurrent fractures. Current clinical tools, such as dual energy X-ray absorptiometry (DXA), provide only limited information about the bone's ability to resist fatigue, as they neglect the matrix-level properties critical for fracture resistance. Bone water, especially matrix-bound water, plays a central role in toughness and stiffness, and its depletion has been linked to fragility in multiple conditions. The goal of this study was to evaluate whether whole-bone imaging of bound and pore water using ultrashort echo time MRI (UTE-MRI)[6], combined with cortical structural measures from high-resolution peripheral quantitative computed tomography (HR-pQCT) and localized compositional mapping by Fourier transform near-infrared spectral imaging (FT-NIR), can reveal relationships between matrix hydration, tissue composition, and mechanical damage under low-cycle fatigue.

METHODS: Bilateral cadaveric tibiae (n=22) from 11 donors (9 F, 2 M) were obtained through the IUSM Anatomical Education Program. Fresh-frozen whole tibiae were imaged using high-resolution peripheral quantitative computed tomography (HR-pQCT, voxel size: 60.7 µm) to assess cortical architecture and density, and dual-echo ultrashort echo time MRI (UTE-MRI, 3T Siemens; TE1=0.04 ms, TE2=2.8 ms; voxel size: 1.07 mm) to quantify matrix-bound and pore water. The left tibia (n=11) was subjected to low-cycle fatigue loading in four-point bending (Instron 6800 Series) using a lower span equal to one eighth the tibial length (1:8 span ratio), with the upper span defined as one-third of the lower span, with the tibia's medial surface in tension. Maximum force was set to achieve an estimated 80 MPa surface stress, calculated from second area moments (CT-derived) and medial-lateral diameters. Each specimen underwent 10 triangular waveform cycles (strain rate = 0.001 /s, 20–100% max force; 20% minimum to prevent slip) to induce subcritical damage. Acoustic emission (AE) was recorded during four-point bending using a sensor mounted on the lateral surface (Physical Acoustics Corporation). AE signals capture the release of elastic energy associated with microdamage events, such as microcrack initiation and propagation within bone tissue. Signals were sampled at 5 MSPS, pre-amplified by 40 dB, and processed with a 40 dB activation threshold and a 20–50 kHz frequency range. UTE-MRI was repeated following fatigue.

Bilateral tibiae were then sectioned at three anatomically matched shaft regions spanning areas of high (within upper spans) and low mechanical stress (distal to the lower support), mirrored across left and right tibiae for paired comparisons. Sectioned regions underwent Fourier Transform Near Infrared Spectral Imaging (FT-NIR SI, 25 µm) for highly localized compositional analysis. Specific absorbances quantified included matrix water (5200, 6900 cm^{-1}), collagen (4600, 5800–6000 cm^{-1}), non-collagenous proteins (4500–4800 cm^{-1}), and lipids (4300–4400, 5700–5800 cm^{-1}).

Table 1. Structural parameters and mechanical test inputs for tibiae.

Length (cm)	Midshaft Architecture		Mech. Test Inputs	
	Ct.Th (mm)	I(mm^4)	Peak Force (N)	Disp. Rate (m/s)
37.2 ± 2	3.8 ± 1.4	7.25 E-09 ± 3.6 E-09	1931.98 ± 575.1	0.28 ± 0.03

RESULTS: There were no side-to-side differences between right and left tibiae in length, cortical thickness, or second moment of inertia. Average structural parameters and the corresponding mechanical test inputs are summarized in **Table 1**. During four-point bending (**Fig. 1A**), acoustic emission (AE) demonstrated the highest number of hits during the first loading cycle, with cumulative hits continuing to increase across subsequent cycles but with fewer new events per cycle (**Fig. 1B**). Representative UTE-MRI baseline images are shown in **Figure 1C**, including bound water index (BWI) and HR-pQCT cortical structure. FT-NIR spectral imaging from non-loaded right tibiae demonstrated regional differences in water absorbance, with the lowest water content observed at the midshaft compared to proximal and distal cross-sections (**Fig. 1D**). Quantitative analysis of BWI and porosity index (PI) from UTE-MRI pre- and post-fatigue, along with FT-NIR results from fatigued tibiae, is ongoing.

DISCUSSION: This study establishes the feasibility of integrating UTE-MRI, HR-pQCT, and FT-NIR to assess bone hydration, structure, and composition in the context of fatigue loading. While quantitative MRI analyses are ongoing, the successful acquisition of whole-bone water maps alongside compositional and mechanical data demonstrates a framework for linking matrix-level properties to fatigue damage. This study provides a foundation for future in vivo work aimed at implementing water-based imaging biomarkers to assess fracture risk, particularly stress fracture risk.

CLINICAL RELEVANCE: Stress fractures remain difficult to detect early because current clinical imaging lacks sensitivity to tissue-level properties. UTE-MRI, and matrix-bound water in particular, may represent an important adjuvant to current evaluation methods in people at risk, though additional work is needed to establish its clinical utility.

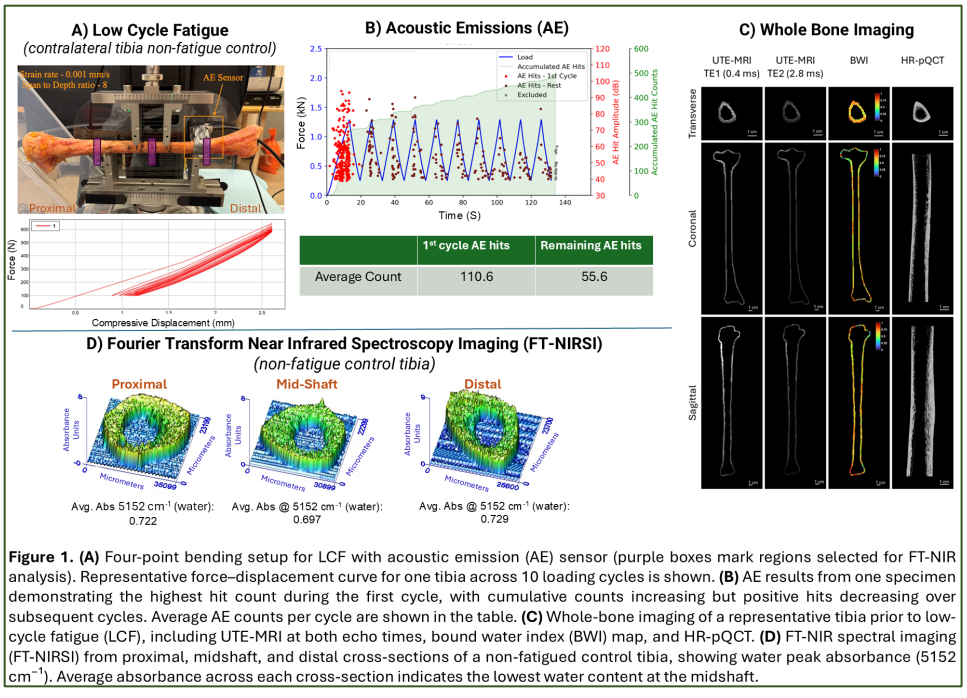

Figure 1. (A) Four-point bending setup for LCF with acoustic emission (AE) sensor (purple boxes mark regions selected for FT-NIR analysis). Representative force–displacement curve for one tibia across 10 loading cycles is shown. **(B)** AE results from one specimen demonstrating the highest hit count during the first cycle, with cumulative counts increasing but positive hits decreasing over subsequent cycles. Average AE counts per cycle are shown in the table. **(C)** Whole-bone imaging of a representative tibia prior to low-cycle fatigue (LCF), including UTE-MRI at both echo times, bound water index (BWI) map, and HR-pQCT. **(D)** FT-NIR spectral imaging (FT-NIRSI) from proximal, midshaft, and distal cross-sections of a non-fatigued control tibia, showing water peak absorbance (5152 cm^{-1}). Average absorbance across each cross-section indicates the lowest water content at the midshaft.